SUPPLEMENTARY INFORMATION

Genotyping. Tail tissues were collected by dissecting ~0.2 cm of tail at P10 (for behavioral experiments) or at the terminal time point for all other experiments. Genotyping was performed with Mouse Genotype. The *Ddx3x* alleles were identified using two sets of primers. Primers 4539 (5'- GATGCATACAACATCCTGAACC-3') and 4540 (5'-GCCCTGACTTCAAACCTCTTAG-3') yielded a 744 bp, a 899 bp, or a 412 bp amplicon for the wild type (*Ddx3x*$^{+}$), floxed (*Ddx3x*^{flox}), or Δexon2 (*Ddx3x*$^{-}$) alleles, respectively [1]. Primers 4540 (5'-GCCCTGACTTCAAACCTCTTAG-3') and 4541 (5'-CTTGCTGTACTTCCTCCACTCTG-3') yielded a 515 bp or a 618 bp amplicon, for the *Ddx3x*$^{+}$ or *Ddx3x*^{flox}, respectively [1]. The Sox2-Cre transgene was amplified using primers 4572 (5'-AATGGTTTCCCGCAGAACCT-3') and 4573 (5'-GCATTGCTGTCACTTGGTCG-3'). To confirm male identity, the *Sry* locus was amplified using 4598 (5'-TGGCAGCCTGTTGATATCCC-3') and 4599 (5'-CTGAGGTGCTCCTGGTATGG-3') [1]. The Emx1-Cre transgene was detected using primers 49245 (5'-CAACGGGGAGGACATTGA-3'), 49246 (5'-CAAAGACAGAGACATGGAGAGC-3') and 51072 (5'-TCGATAAGCCAGGGGTTC-3') to yield a 315 bp or a 195 bp amplicon, for the WT or mutant alleles, respectively [2]. Given the occurrence of germline recombination observed in Cre driver lines designed for the central nervous system [3], we performed genotyping on both non-targeted tissues (tail, ear, leg muscle, heart, liver and cerebellum) alongside the targeted tissue (cortex) in a cohort of *Emx1-Ddx3x* mutants. In *Emx1-Ddx3x*$^{-/y}$ males, non-targeted tissues harbored only the *Ddx3x*^{flox} allele, while the *Ddx3x*$^{-}$ allele was detected only in the cortex, as intended. In *Emx1-Ddx3x*$^{+/-}$ females, *Ddx3x*$^{+}$ and *Ddx3x*^{flox} alleles were detected in non-targeted tissues, while the *Ddx3x*$^{+}$ and *Ddx3x*$^{-}$ alleles were detected exclusively in the cortex, as expected. In a minority of cases, the *Ddx3x*$^{-}$ allele was identified jointly with the *Ddx3x*$^{+}$ and *Ddx3x*^{flox} alleles only in ear and/or tail samples of *Emx1-Ddx3x*$^{+/-}$ females (but not in Cre-negative mice), in line with previous observations [3] that suggest a possible mosaic recombination in ear/tail tissues.

Testing of developmental milestones. Testing was performed as reported previously [1,4]. To control for litter size effects, litters were homogenized and limited to 6 pups per dam by adding excess pups to smaller litters on P1, whenever possible. Pups were identified by hind-paw tattoo using a nontoxic animal tattoo ink (Animal Identification & Marking Systems Inc) inserted subcutaneously through a 30-gauge hypodermic needle tip into the center of the paw. Testing occurred at the same time of day, every day from P1 to P21 (weight was taken

until P27). Individual pups were removed from the litter and placed on cotton pads under a heating lamp to maintain a temperature of 28ºC throughout the testing. All tasks were conducted quickly and capped at 30 seconds to minimize maternal separation. The animals used for testing of developmental milestones were not employed for adult testing, to avoid confounding effects from maternal separation. All four genotypes were tested on the same day in randomized order by an experimenter blind to the animals' genotype. All data were scored and analyzed blind to the genotype. Details for each test are indicated below.

Physical Milestones. Body weight was taken between P1 and P28, and was measured in grams. Fur and skin development was monitored between P1 and P15 and scored as follows: 1 = bright red, 2 = nude/pink, 3 = nude/grey, 4 = grey/fuzzy on back and shoulders, 5 = black hair on back/grey fuzzy belly, 6 = black hair fully covering body. Ear development was monitored between P1 and P9, and was scored as follows: 0 = ear bud not detached from pinna, 1 = ear flap detached from pinna. Top and bottom tooth eruption was monitored between P7 and P18, and separately scored as follows: 0 = incisors not visible, 1 = incisors visible but not erupted, 2 = incisors fully erupted. Eye opening was monitored between P10 and P20, and scored as follows: 0 = eyes fully closed, 1 = eyes partially open, 2 = eyes fully open.

Sensory Milestones. Cliff aversion reflex was measured between P2 and P14. The reflex was assessed by placing the mouse on the edge of an opaque plexiglass platform 30 cm high and was scored as follows: 0 = fall off, 1 = stay, 2 = turn away. Additionally, the latency to turn away from the edge was recorded. Forelimb grasp reflex was measured between P4 and P13. The reflex was tested by stimulating the front paws with a small plastic zip tie. The responses were scored as follows: 0 = no response, 1 = paws folding in response to stimulation, 2 = paws grasping zip tie in response to stimulation, 3 = paws grasping strong enough to hold for at least 1 sec when hanging. Auditory startle response was measured between P6 and P18. The pups were exposed to an 80 dB click 30 cm above. The reflex was considered present (score 1) when the pup startled immediately after the click. Ear twitch reflex was assessed between P7 and P15 by stimulating each ear with the tip of a cotton swab pulled to form a filament. The reflex was considered present (score 1) when the ear moved in response to the stimulation. Vibrissa placing reflex (P5-15) and visual placing (P13-18) were tested by slowly lowering the pup by the tail onto a flat surface. The vibrissa response was considered present (score 1) when the pup reached out forward with its forepaws to prepare to place itself when its whiskers touched the surface.

The visual response was considered present (score 1) when the pup reached out with its forepaws to prepare to place itself when it saw the surface close below, before the vibrissa touched the surface.

Motor Milestones. Surface righting reflex was measured between P2 and P13 by placing the pup supine on a flat surface and recording the latency to turn over to a prone position with all 4 paws on the ground. The negative geotaxis behavior (P2-16) was tested by placing the pup head down on a mesh covered platform at a 45-degree angle. Scoring was as follows: 0 = fall off, 1 = stay/move down/walk down, 2 = turn and stay, 3 = turn, move up, and stay, 4 = turn and move up to the top. Air righting reflex (P8-19) was tested by dropping the pup from a supine position 30 cm above a padded surface and scored as follows: 0 = fall on back, 1 = fall onto side, 2 = fall onto all 4 paws, successfully righting themselves in the air. Locomotor activity in open field crossing was tested between P8 and P20 by recording the latency to exit a 13 cm diameter circle when placed in the center. Rod suspension skills were measured between P11 and P20 by recording the latency to stay suspended on a 3 mm rod, 30 cm above a padded surface. Hind limbs suspension skills were measured between P2 and P12 by recording the latency to stay suspended on the edge of a 50 mL falcon tube by the hind limbs. Grip strength was monitored between P5 and P14 by placing the mouse on a mesh grid and rotating the grid from a horizontal to vertical position. The angle of the grid when the mouse fell off was recorded.

Gait analyses. Testing was performed as described previously [1]. The paws of P19, P22, P30 mice were painted in non-toxic and water-washable dyes (back paws in blue and front paws in red). Mice were then placed on an absorbent paper runway and encouraged to walk in a straight line. Paws were wiped clean with water. Measures were taken as indicated in **Fig. S10A**.

Handling and assessment of physical appearance and spontaneous activity prior to behavioral testing. On day 1, physical appearance was monitored in the housing room. Body weight (g) was taken, and body length (cm) was measured from the base of the tail to the tip of the nose. Coat appearance was visually examined on a scale: 0 = ungroomed 0-25%, 1 = partial grooming 25-50%, 2 = semi-groomed 50-75%, 3 = groomed 75-100%. Skin color of footpads was visually measured on a scale: 0 = pink, 1 = purple, 2 = other. Whisker barbering was visually scored on a scale: 0 = normal, 1 = shortened/missing. Patches of missing fur on face and on body are visually measured separately on a scale: 0 = none, 1 = some, 2 = extensive. Wounding was visually measured

on a scale: 0 = none, 1 = signs of previous wounding, 2 = slight wounds present, 3 = moderate wounds present, 4 = extensive wounds present.

On day 2, spontaneous general activity was monitored for 5 minutes by placing the animal in a 1000 mL jar in the behavioral suit. The following parameters were measured: grooming time (sec), number of rears, number of jumps, body position (scored on a scale: 0 = completely flat, 1 = lying on side, 2 = lying prone, 3 = sitting or standing, 4 = rearing on hind limbs, 5 = repeated vertical leaping), spontaneous activity (scored on a scale: 0 = none/resting, 1 = casual scratch/groom, slow movement, 2 = vigorous scratch/groom, moderate movement, 3 = vigorous rapid movement, 4 = extremely vigorous rapid movement), respiration rate (scored on a scale: 0 = gasping, 1 = slow and shallow, 2 = normal, 3 = hyperventilation), tremor (scored on a scale: 0 = none, 1 = mild, 2 = marked), urination (scored on a scale: 0 = none, 1 = little, 2 = moderate, 3 = extensive), and defecation (number of fecal boli). After the 5 minutes observation, the mice were briskly transferred to an empty cage for observation by tipping the beaker over the cage. The following parameters were monitored: transfer arousal (scored on a scale: 0 = coma, 1 = prolonged freeze, slight movement, 2 = brief freeze, then active movement, 3 = no freeze, stretch attends, 4 = no freeze, immediate movement), eyelid closure (scored on a scale: 0 = eyes wide open, 1 = eyes half open, 2 = eyes closed), spontaneous piloerection (0 = none, 1 = coat standing on end), gait (0 = normal, 1 = fluid but abnormal, 2 = slow and halting, 3 = limited movement only, 4 = incapacitated), pelvic elevation (scored on a scale: 0 = markedly flattened, 1 = barely touches, 2 = normal, 3 = elevated), and tail elevation (scored on a scale: 0 = dragging, 1 = horizontally extended, 2 = less than 30° elevation, 3 = 30-60° elevation, 4 = 60-90° elevation).

On day 3, reflexes and reactions were observed in the housing room. Touch escape was measured by stroking a finger on the mouse's back, starting lightly and getting firmer, and scored on a scale: 0 = no response, 1 = escape response to firm stroke, 2 = escape response to light stroke, 3 = escape response to stroke approach. Trunk curl was measured by holding the mouse by the tail 30 cm above the surface and noting the presence or absence of a trunk curl. Body tone was measured by compressing both sides of the mouse between the experimenter's thumb and index finger and scored on a scale: 0 = flaccid, 1 = slight resistance, 2 = extreme resistance. Startle reflex was measured by an 80 dB click 30 cm above the mouse and scored on a scale: 0 = none, 1 = ear/head twitch, 2 = jump. Positional passivity was measured on a scale: 0 = Struggles when restrained

by tail, 1 = Struggles when restrained by neck (finger grip), 2 = Struggles when held supine (on back), 3 = Struggles when restrained by hind legs, 4 = Does not struggle.

On day 4, reflexes and reactions were observed in the housing room. The pinna reflex was tested by stimulating each ear with the tip of a cotton swap pulled to form a filament. The reflex was considered present when the ear moved in response to the stimulation. Salivation and lacrimation were observed separately and scored on a scale: 0 = none, 1 = mild, 2 = marked. Provoked biting was tested by inserting a 3 mm rod between the teeth at the side of the mouse's mouth and scored on a scale: 0 = none, 0.5 = nibble, 1 = biting. Vocalization was considered present if the mouse was audible squeaking during handling.

On day 5, motor reflexes were observed in the housing room. Forelimb placing was tested by slowly lowering the mouse by the tail onto a flat surface and scored on the following scale: 0 = none, 1 = reaching after nose contact, 2 = reaching after vibrissa contact, 3 = reaching after visually seeing surface, before vibrissa touch the surface. Hind limb placing was tested by having the mouse grip a vertical mesh grid with its forepaws while the experimenter held its tail so that its body is horizontal. When the tail was released, the response was scored on a scale: 0 = grabs but falls, 1 = grabs but hangs, 2 = grabs and pulls body onto the grid. Negative geotaxis was tested by placing the mouse head down on a mesh covered platform at a 45° angle and scored on a scale: 0 = fall off, 1 = stays, 2 = moves but does not turn 3 = turn and stays, 4 = turn and climbs up. The placing, hind limb placing, and negative geotaxis tasks were repeated three times in that order and the average of the three trials were used for analysis. The inverted screen task was tested by placing the mouse on a mesh platform, which was then inverted 180° 60 cm over a padded surface. The time that the mouse fell from an upside-down position was recorded (60 sec cutoff).

Constraint analyses. Constraint metrics were obtained from the Genome Aggregation Consortium (gnomAD), Cambridge, MA (URL: https://gnomad.broadinstitute.org) [gnomAD v2.1.1] [5]. We used the loss-of-function observed/expected upper bound fraction (LOEUF) metrics [5]. For the partitioning of genes in LOEUF deciles, deviation from the distribution observed for all genes was evaluated using Kolgomorov-Smirnov test (ks.test, R).

Enrichment analyses. The DDG2P genes were defined as the 1,338 unique genes with the "brain" term included in "organ specificity" in the Developmental Disorders Genotype-Phenotype Database (DDG2P, https://www.deciphergenomics.org/ddd/ddgenes, Sept 2023) [6]. The ASC genes were defined as the 185 genes

identified by the Autism Sequencing Consortium [7]. The EPI genes were defined as 65 unique genes compiled by merging the known genes associated with dominant epilepsy disorders included in Table S5 of the Epi4K study [8] and the known genes associated with dominant developmental epileptic encephalopathy syndromes included in Table S3 of Heyne et a. (2018) [9], as indicated by the Epi25 Collaboration [10]. The FMRP targets are defined as the genes encoding the 842 FMRP mRNAs [11]. The RBFOX targets are defined as the 1,048 genes mapped with significant RBFOX1/2/3 HITS-CLIP peaks in the exon or CDS region [12]. The CELF4 targets are defined as the top 431 iCLIP targets of CELF4 [13]. We used as input sets the human orthologues of the murine genes encoding the 193 proteins differentially expressed in *Ddx3x*$^{+/+}$ vs *Ddx3x*$^{+/y}$ neurons, 182 proteins differentially expressed in *Ddx3x*$^{+/-}$ vs *Ddx3x*$^{+/+}$ neurons, 98 proteins differentially expressed in *Ddx3x*$^{-/y}$ vs *Ddx3x*$^{+/y}$ neurons, and 498 proteins differentially expressed in *Sox2-Ddx3x*$^{+/-}$ vs *Sox2-Ddx3x*$^{+/+}$ synaptoneurosomes. We used the DDG2P genes, ASC genes, EPI genes, FMRP targets, RBFOX targets, and CELF4 targets as target sets, and all the proteins detected in the proteomics datasets as background sets. For each comparison between the input and target sets, we first constructed the empirical distribution by sampling the same number of genes as in the input set from the background set 10,000 times. The empirical *P*-value was then computed by calculating the number of sampled gene lists that had at least as many overlapping genes with the target sets as the input set, divided by 10,000 iterations, as in previous analyses [14].

Sex biased expression in human tissues. For the transcriptomic analyses of X-linked genes in Fig. S1A, we extracted the chromosomal position of the murine genes encoding the 182 proteins differentially expressed in *Ddx3x*$^{+/-}$ compared to *Ddx3x*$^{+/+}$ neurons from ENSEMBL Genome Browser, and then filtered for X-linked genes (*Ddx3x* and *Ubl4a*). We then interrogated the log(fold change) in females vs males tissues based on 5,500 transcriptomes from 449 individuals spanning 29 tissues in the Genotype-Tissue Expression project (GTEx, v6p release), extracted from Table S2 of Tukiainen et al. (2017) [15]. For the analyses of sex bias in expression in Fig. S1B, we extracted the list of the 500 top human genes with sex differences in expression in the brain region “BRNCTXA” in GTEx v8 release, alongside the MASH Statistics (log2 FC) and LFSR (local false sign rate), as in Table S2 of Oliva et al., (2020) [16].

Puromycilation experiments. Prior to puromycin administration, half of the conditioned medium was collected from the neurons and stored into microcentrifuges tubes. Neurons were then treated with 10 µg/ml of Puromycin

(Sigma-Aldrich, #P8833) for 10 minutes in the incubator. As a control, a set of plates were pre-treated with 60 µM of cycloheximide (Sigma-Aldrich, # C7698) for 15 minutes in the incubator prior to puromycin administration. At the end of the puromycin treatment, the medium was removed and replaced by the medium isolated prior to treatment for 30 minutes in the incubator. Plates were then placed on ice, washed three times with ice-cold 1X PBS supplemented EDTA-free protease inhibitor cocktail (Sigma-Aldrich, #1183617001, 1 tablet in 10 mL) and phosphatase inhibitor cocktail (Sigma-Aldrich, #P0044, 1:1000), cells were harvested with 200 µL of 1X PBS supplemented with protease and phosphatase inhibitors and stored at -80°C. Cells were centrifuge for 3 minutes at 800 g at 4°C, supernatants were discarded and pellets were then lysed with 200 µl of RIPA buffer (Thermo Scientific, #89901) supplemented with protease and phosphatase inhibitors. Lysates were vortexed for 10 sec every 5 minutes and kept on ice for 30 minutes. Samples were then centrifuged for 10 minutes at 13,800 g at 4°C. Pellets were discarded and the supernatants were transferred to new microcentrifuge tubes.

Western blotting. Protein concentration was quantified using the BCA protein assay (Thermo Scientific, #23225). Protein samples were supplemented with Laemmli's sample buffer 4X (Biorad, #1610747) containing 5% (v/v) of 2-Mercaptoethanol (Sigma-Aldrich, #M6250) and then boiled at 95°C for 5 minutes in a dry bath. 5 µg (puromycilation experiment) or 15 µg of proteins (DDX3X expression) were resolved on 4–20% mini TGX precast protein gels (Biorad, #4561094) at a constant voltage of 120 V for 120 minutes. Gels were transferred onto PVDF membranes (Biorad, #1704156) using the Trans-blot turbo transfer system (Biorad, #1704150). Membranes were incubated with 5 mL of EveryBlot blocking buffer (Biorad, #12010020) for 1 hour at RT with gentle shaking. After blocking, membranes were incubated with a rabbit anti-DDX3X polyclonal antibody (Thermo Fisher Scientific, #A300-474A, 1:1000), a mouse monoclonal antibody raised against the first 80 residues at the N-terminus of DDX3Y which recognizes both DDX3X and DDX3Y (Sigma-Aldrich, #WH0008653M1, 1:1000), a mouse anti-puromycin monoclonal antibody (Sigma-Aldrich, #MABE343, 1:1,000), a mouse anti-ribosomal protein S5 antibody (A-8, Santa Cruz, sc-390935, 1:200), a mouse anti-ribosomal protein L36a antibody (43-A, Santa Cruz, sc-100831, 1:500), a mouse anti-ribosomal protein L11 antibody (3A4A7, Invitrogen, #37-3000, 1:25), a mouse anti-eIF3K antibody (F-4, Santa Cruz, sc-393234, 1:50), or a rabbit anti-GAPDH monoclonal antibody (Sigma-Aldrich, # ZRB374, 1:5,000) in 5 mL of EveryBlot blocking buffer overnight at 4°C with gentle shaking. The next day, membranes were washed three times with 1X Tris buffered saline

((TBS, Boston BioProducts, #BM301)/0.05% (v/v) Tween 20 (Acros Organics, #EW-88248-22, 1X TBST)) for 5 minutes each time, and then incubated with a goat anti-rabbit HRP-conjugated antibody (Sigma-Aldrich, #12-348, 1:1,000), a goat anti-mouse HRP-conjugated antibody (Sigma-Aldrich, #12-349, 1:2,000), a goat anti-rabbit StarBright Blue 700 antibody (Biorad, #12004162, 1:2,500), or a goat anti-mouse StarBright Blue 520 antibody (Biorad, #12005867, 1:2,500) in 1X TBST for 1 hour at RT with gentle shaking. Membranes were washed three times with 1X TBST and then developed with the ChemiDoc MP Imaging System (Biorad, #12003154) using the ECL detection kit (Thermo Fisher Scientific, #32106; puromycilation experiment) or the fluorescent detection (DDX3X expression).

Coomassie blue staining. After puromycin immunodetection, membranes were rinsed three times with double-distilled water for 5 minutes each time and exposed for 10 minutes at RT with the GelCode blue staining reagent (Thermo Fisher Scientific, #24590) under gentle shaking to evaluate the levels of transferred proteins. Membranes were then incubated with a 10% methanol/80% water/10% acetic acid destaining solution for 1 hour at RT under gentle shaking. After destaining, membranes were rinsed three times with double-distilled water for 5 minutes each time and dried at RT. Membranes were then imaged with the ChemiDoc MP Imaging System using the colorimetric detection.

SUPPLEMENTARY FIGURES

Supplementary Figure 1. Distribution of the dendritic segments examined for the dendritic spine analyses. A) Distribution of dendritic spines across dendrite hierarchies. The plot shows the number of dendritic spines in 10 μm segments as a function of the distance from the soma for primary, secondary, and tertiary dendrites. Data are pooled across all five genotypes. **B) Distribution of dendritic spines as a function of dendrite thickness.** The plot shows the number of dendritic spines in 10 μm segments as a function of the distance from the soma for thin (0.2-0.5 μm caliber) and thick (0.5-0.8 μm caliber) dendrites. Data are pooled across all five genotypes. **C) Distribution of dendritic segments examined across dendrite hierarchies in each genotype.** The histogram shows the distribution of 10 μm segments analyzed stratified by their hierarchy (primary, secondary, and tertiary dendrites). **D) Distribution of dendritic segments based on dendrite thickness in each genotype.** The histogram shows the distribution of 10 μm segments analyzed stratified by their diameter. Source data are provided as a Source Data file.

Supplementary Figure 2. *Ddx3x* regulates the formation of dendritic spines especially on secondary and thin dendrites. A) Density of dendritic spines across dendrite hierarchies. The plot shows the number of dendritic spines in 10 μm segments for primary, secondary, and tertiary dendrites of *Ddx3x*$^{+/+}$, *Ddx3x*$^{+/-}$, *Ddx3x*$^{-/}$, *Ddx3x*$^{+/y}$, or *Ddx3x*$^{-/y}$ neurons. **B) Density of dendritic spines stratified by dendrite diameter.** The plot shows the number of dendritic spines in 10 μm segments for thick (0.5-0.8 μm caliber) or thin (0.2-0.5 μm caliber) dendrites from *Ddx3x*$^{+/+}$, *Ddx3x*$^{+/-}$, *Ddx3x*$^{-/}$, *Ddx3x*$^{+/y}$, or *Ddx3x*$^{-/y}$ neurons. **Statistics**: Panels A-B, two-way ANOVA, followed by Student's t test with Benjamini-Hochberg correction. In all panels, data were collected blind to genotype and sex; *n* is shown in legend as number of neurons (and number of embryos); mean ± SEM; outliers shown as ⊗; **P*-value<0.05, ***P*-value<0.01, ****P*-value<0.001. Source data are provided as a Source Data file.

Supplementary Figure 3. Associations between differentially expressed proteins and neurodevelopmental disorders. A) *DDX3X* escapes X chromosome inactivation, while *UBL4A* does not. The heatmap shows the log2 fold change in female vs. male tissues, based on 5,500 transcriptomes from 449 individuals across 29 human tissues [15]. *DDX3X* shows consistent female bias in expression, while *UBL4A* shows no bias, suggesting that in humans it undergoes X chromosome inactivation. **B) Genes with higher expression**

in female murine neurons and human female cortices. The plot shows the 500 genes (gray) with sex differences in expression in the cortex distributed based on their MASH Statistics, as in [16], without including *XIST*. The 5 genes, including *DDX3X*, with differential expression in female neurons compared to male neurons, are shown in red. **C) Genomic constraints of human orthologues of gene differential expressed based on sex or *Ddx3x* dosage.** The plots show the distribution based on the loss-of-function observed/expected upper bound fraction (LOEUF) metrics [5] for all genes in gnomAD (grey), the human orthologues of the 193 proteins differentially expressed in *Ddx3x*$^{+/+}$ vs *Ddx3x*$^{+/y}$ neurons (black), the human orthologues of the 182 proteins differentially expressed in *Ddx3x*$^{+/-}$ vs *Ddx3x*$^{+/+}$ neurons (blue), the human orthologues of the 98 proteins differentially expressed in *Ddx3x*$^{-/y}$ vs *Ddx3x*$^{+/y}$ neurons (gold), and the human orthologues of the 498 proteins differentially expressed in *Sox2-Ddx3x*$^{+/-}$ vs *Sox2-Ddx3x*$^{+/+}$ synaptosomes (coral). **D) Enrichment results for association to neurodevelopmental disorders, including RNA-binding proteins associated with ID and/or ASD.** The heatmap shows the permutation-based empirical *P*-value of the enrichment that the human orthologues of the 193 proteins differentially expressed in *Ddx3x*$^{+/+}$ vs *Ddx3x*$^{+/y}$ neurons (black), the human orthologues of the 182 proteins differentially expressed in *Ddx3x*$^{+/-}$ vs *Ddx3x*$^{+/+}$ neurons (blue), the human orthologues of the 98 proteins differentially expressed in *Ddx3x*$^{-/y}$ vs *Ddx3x*$^{+/y}$ neurons (gold), and the human orthologues of the 498 proteins differentially expressed in *Sox2-Ddx3x*$^{+/-}$ vs *Sox2-Ddx3x*$^{+/+}$ synaptosomes (coral) show in DDG2P genes [6], ASC genes [7], EPI genes [8-10], FMRP targets [11], RBFOX targets [12], and CELF4 targets [13]. The number of overlapping genes is indicated in each tile. **E) Nominal overlap of proteins across the four proteomics datasets,** namely the proteins differentially expressed in *Ddx3x*$^{+/+}$ vs *Ddx3x*$^{+/y}$ neurons (black), the proteins differentially expressed in *Ddx3x*$^{+/-}$ vs *Ddx3x*$^{+/+}$ neurons (blue), the proteins differentially expressed in *Ddx3x*$^{-/y}$ vs *Ddx3x*$^{+/y}$ neurons (gold), and the proteins differentially expressed in *Sox2-Ddx3x*$^{+/-}$ vs *Sox2-Ddx3x*$^{+/+}$ synaptosomes (coral). **Statistics**: Panel C, Kolgomorov-Smirnov test; Panel D, empirical permutation analyses. **P*-value<0.05, ***P*-value<0.01, ****P*-value<0.001. Source data are provided as a Source Data file.

Supplementary Figure 4. Validation of the viral-mediated infection strategy and proteomic results in Fig. 4. A) Western blot of DIV9 cortical neurons from *Ddx3x*$^{+/+}$ (lanes 1-2), *Ddx3x*$^{+/y}$ (lanes 3-4), *Ddx3x*$^{flox/flox}$ (lanes 5-6), or *Ddx3x*$^{flox/y}$ (lanes 7-8) embryos infected with the AAV8-Ef1a-mCherry-IRES-Cre as shown in Fig. 4A. The resulting *Ddx3x*$^{-/-}$ (lanes 5-6) or *Ddx3x*$^{-/y}$ (lanes 7-8) neurons lack DDX3X expression. *Ddx3x*$^{-/y}$ (lanes 7-8) neurons show expression of DDX3Y, as detected by an antibody that recognizes both DDX3X and DDX3Y (see

Methods). **B)** Western blot for RPS5, RPL11, RPL32A, eIF3K, and DDX3X on *Ddx3x*$^{+/+}$ (lanes 1-5) and *Ddx3x*$^{+/-}$ (lanes 6-10) DIV9 cortical neurons, obtained as in Fig. 4A. **C)** Quantification of the Western blot data shown in panel B. The expression of RPS5, RPL11, RPL32A, eIF3K, and DDX3X normalized over GAPDH is compared between *Ddx3x*$^{+/+}$ and *Ddx3x*$^{+/-}$ neurons. **Statistics**: Student's t test; *n* is shown in legend as number of embryos; mean ± SEM; ⊗ indicate outliers; **P*-value<0.05. Source data are provided as a Source Data file.

Supplementary Figure 5. Sex and *Ddx3x* dosage do not result in gross changes in total protein synthesis. A) Experimental design. DIV9 *Ddx3x*$^{+/+}$, *Ddx3x*$^{+/-}$, *Ddx3x*$^{+/y}$ neurons obtained as outlined in the scheme in Fig. 4A were subjected to a 10-min pulse of puromycin (PURO) or vehicle (VEH), followed by a 30-min chase. As a control, DIV9 *Ddx3x*$^{+/+}$, *Ddx3x*$^{+/-}$, *Ddx3x*$^{+/y}$ neurons were pre-treated for 15 minutes with protein synthesis inhibitor cycloheximide (CHX), followed by the PURO pulse-chase (CHX+PURO). **B-C) Puromycin-based assay to detect nascent polypeptides.** Upper panel, Western blot with an anti-puromycin antibody to detect newly synthesized proteins during the 15-min puromycin pulse; lower panel, Coomassie staining to detect overall proteins. Lane 1, VEH control; lane 2-4, neuronal lysates from DIV9 *Ddx3x*$^{+/+}$, *Ddx3x*$^{+/-}$, *Ddx3x*$^{+/y}$ neurons after the puromycin pulse-chase experiment shown in panel A (PURO); lanes 5-7, neuronal lysates from DIV9 *Ddx3x*$^{+/+}$, *Ddx3x*$^{+/-}$, *Ddx3x*$^{+/y}$ neurons after the puromycin pulse-chase experiment with prior CHX treatment shown in panel A (CHX-PURO). **C) No changes in global protein synthesis were detected in *Ddx3x* haploinsufficient neurons.** The plot shows the quantification of the anti-puromycin signal over the total Coomassie across the three genotypes. **Statistics**: In all panels, data were collected blind to genotype and sex; *n* is shown in legend as number of embryos; mean ± SEM. Source data are provided as a Source Data file.

Supplementary Figure 6. Female cortical neurons in culture have more nucleoli in a *Ddx3x*-dependent manner. A) DIV9 DDX3X-expressing cortical neurons cultured from E15 embryos as shown in Fig. 1A express CTIP2. Representative confocal images of sparsely transfected DIV9 cultures stained for DDX3X (cyan), CTIP2 (green) or mCherry (red). **B) Nucleoli staining of *Ddx3x* mutant neuronal cultures**. Using the experimental design depicted in Fig. 1A, we generated sparsely labeled control female neurons (*Ddx3x*$^{+/+}$), haploinsufficient female neurons (*Ddx3x*$^{+/-}$), control male neurons (*Ddx3x*$^{+/y}$), and null male neurons (*Ddx3x*$^{-/y}$). Immunostaining for mCherry (red), Fibrillarin (FBL, green), and Hoechst (blue) on DIV9 cortical neurons, showing the sparse labeling and the FBL-stained nucleoli. **C) Nucleoli volume in control female, control male, and**

***Ddx3x* male and female mutant neurons.** The plot shows the empirical cumulative distribution function (cumulative probability) of the nucleoli volume across the four genotypes. **D) Total nucleolar in control female, control male, and *Ddx3x* male and female mutant neurons.** Plot showing the sum volume of all the nucleoli in the nucleus across the four genotypes. **E) Nuclear volume in control female, control male, and *Ddx3x* male and female mutant neurons.** Plot showing the nuclear volume across the four genotypes. **F) Female neurons have more nucleoli than male neurons, but not if *Ddx3x* expression is monoallelic.** The plot shows the number of nucleoli across the four genotypes. **Statistics**: Panel C, Panels D-F, one-way ANOVA, followed by Student's t test with Benjamini-Hochberg correction. In all panels, data were collected blind to genotype and sex; *n* is shown in legend as number of neurons; mean ± SEM; ⊗ indicate outliers; **P*-value<0.05. Source data are provided as a Source Data file.

Supplementary Figure 7. Postnatal physical milestones in *Emx1-Ddx3x* mutant mice. A) *Emx1-Ddx3x* mutant pups do not show a delay in eye opening. The plot shows the eye-opening score over time. **B) *Emx1-Ddx3x* mutant pups do not show a delay in ear development.** The plot shows the pinna detachment score over time. **C) *Emx1-Ddx3x* mutant pups have no changes in bottom tooth development.** The plot shows the score for the eruption of the bottom incisors over time. **D) *Emx1-Ddx3x* null males display a slight delay in top tooth development.** The plot shows the score for the eruption of the top incisors over time. **E) *Emx1-Ddx3x* mutant pups have no changes in fur and skin development.** The plot shows the fur/skin development score over time. **Statistics:** Panels A-E, repeated measure ANOVA as indicated below the plot. Data collected and scored blind to genotype. *n* shown in legend; mean ± SEM. * *P*-value<0.05, *** *P*-value<0.001; ns, non significant. Source data are provided as a Source Data file.

Supplementary Figure 8. Postnatal sensory milestones in *Emx1-Ddx3x* mutant mice. A) *Emx1-Ddx3x* mutant pups do not show a delay in the auditory reflex. The plot shows the response score over time. **B) *Emx1-Ddx3x* female mutants have a delay in the development of forelimb grasp reflex.** The plot shows the grasp reflex score over time. **C) *Emx1-Ddx3x* mutant pups have no changes in the cliff aversion reflex.** The plot shows the score for cliff aversion reflex. **D) *Emx1-Ddx3x* mutant pups have no changes in vibrissae placing.** The plot shows the score for vibrissae placing. **E) *Emx1-Ddx3x* mutant pups have no changes in ear twitch reflex.** The plot shows the score for ear twitch. **F) *Emx1-Ddx3x* mutant pups have no changes in visual**

placing. The plot shows the score for the visual placing score. **Statistics:** Panels A-F, repeated measure ANOVA as indicated below the plot. Data collected and scored blind to genotype. *n* shown in legend; mean ± SEM. * *P*-value<0.05, *** *P*-value<0.001; ns, non significant. Source data are provided as a Source Data file.

Supplementary Figure 9. Postnatal motor milestones in *Emx1-Ddx3x* mutant mice. A) *Emx1-Ddx3x* mutant pups do not show hypotonia. The plot shows the surface righting time over time. **B) *Emx1-Ddx3x* female mutants do not display changes in negative geotaxis.** The plot shows the score in the negative geotaxis test over time. **C) *Emx1-Ddx3x* mutant pups have no changes in rod suspension time.** The plot shows the rod suspension time. **D) *Emx1-Ddx3x* mutant pups have no impairments in developing hindlimb suspension skills.** The plot shows hindlimb suspension time. **E) *Emx1-Ddx3x* null mutant males have a slight delay in acquiring grip strength.** Grip strength was tested by placing pups on a mesh grid and rotating the grid from a horizontal to vertical position. The plot shows the angle of rotation to which pups fall off the grid over time. **F) *Emx1-Ddx3x* null mutant males have a slight delay in acquiring air righting abilities.** The plot shows the air righting time. **G) *Emx1-Ddx3x* null mutant males show a trend toward a delayed trajectory of locomotor activity.** The plot shows the latency to leave the center of an open field. **Statistics:** Panels A-G, repeated measure ANOVA as indicated below the plot. Data collected and scored blind to genotype. *n* shown in legend; mean ± SEM. * *P*-value<0.05, *** *P*-value<0.001; ns, non significant. Source data are provided as a Source Data file.

Supplementary Figure 10. Postnatal trajectories of gait in *Emx1-Ddx3x* mutant mice. A) Gait measures. Gait was analyzed based on footprint patterns of mice walking in a straight line. The back paws were coated in blue paint and the front paws were coated in red paint and the mice were released onto a strip of paper placed in a runway. The different parameters measured to assess gait are shown. Measures were taken at P19, P22, and P30. **B) *Emx1-Ddx3x*$^{+/-}$ female mutants show a persistent increase in the distance between the back paws**, when compared with control *Emx1-Ddx3x*$^{+/+}$ females. **C) *Emx1-Ddx3x*$^{-/y}$ male mutants show a persistent increase in the distance between the fore paws**, when compared with control *Emx1-Ddx3x*$^{+/y}$ males. **D-E) *Emx1-Ddx3x* mutants mice show no alterations in the sway distance (D) or the length of the left stride (E)**. **F) *Emx1-Ddx3x*$^{+/-}$ female mutants show a persistent increase in the length of the right stride**, when compared with control *Emx1-Ddx3x*$^{+/+}$ females. **G-H) *Emx1-Ddx3x* mutants mice show no**

alterations in the distance of the diagonals. **l) *Emx1-Ddx3x*$^{+/-}$ female mutants show a reduction in the number of strides**, when compared with control *Emx1-Ddx3x*$^{+/+}$ females. **Statistics:** Panels B-I, repeated measure ANOVA as indicated below the plot. Data collected and scored blind to genotype. *n* shown in legend; mean ± SEM. * *P*-value<0.05, *** *P*-value<0.001; ns, non significant. Source data are provided as a Source Data file.

Supplementary Figure 11. Spontaneous activity in *Emx1-Ddx3x* mutant mice. A) *Emx1-Ddx3x* mutants do not show changes in the number of rears, as measured during handling. **B) *Emx1-Ddx3x*$^{+/-}$ female mutants, but not male mutants, have reduced number of jumps**, as measured during handling. **C) *Emx1-Ddx3x* mutants do not show changes in provoked biting**, as measured during handling**. D) *Ddx3x*$^{+/-}$ mice display no changes in urination**, as measured during handling. **E) *Ddx3x*$^{+/-}$ mice display no changes in defecation**, as measured during handling. **Statistics:** Panels A and C, *o*ne-way ANOVA for genotype, followed by Student's t test with Benjamini-Hochberg correction; Panels B and E, Kruskal-Wallis test for genotype, followed by Wilcoxon test with Benjamini-Hochberg correction; Panel D, Chi-square test. Data collected and scored blind to genotype. *n* shown in legend; mean ± SEM; ⊗ indicate outliers. * *P*-value<0.05, *** *P*-value<0.001; ns, non significant. Source data are provided as a Source Data file.

Supplementary Figure 12. Additional motor measures in *Emx1-Ddx3x* mutant mice. A) No differences were observed in the number of slips in the balance beam task. B) No differences were observed in the latency, measured as the latency to over 35 frames. **C-D) No differences were observed in the performance on a vertical pole,** either by considering the mean time to turn (C) or the time to descend (D). **Statistics:** Panel A, one-way Welch ANOVA; Panel B and D, one-way Welch ANOVA; Panel C, Kruskal-Wallis test. Data collected and scored blind to genotype. *n* shown in legend; mean ± SEM; ⊗ indicate outliers. * *P*-value<0.05, *** *P*-value<0.001; ns, non significant. Source data are provided as a Source Data file.

SUPPLEMENTARY REFERENCES

1. Boitnott, A., Garcia-Forn, M., Ung, D.C., Niblo, K., Mendonca, D., Park, Y., Flores, M., Maxwell, S., Ellegood, J., Qiu, L.R., et al. (2021). Developmental and Behavioral Phenotypes in a Mouse Model of DDX3X Syndrome. Biol Psychiatry *90*, 742-755. 10.1016/j.biopsych.2021.05.027.
2. Gorski, J.A., Talley, T., Qiu, M., Puelles, L., Rubenstein, J.L., and Jones, K.R. (2002). Cortical excitatory neurons and glia, but not GABAergic neurons, are produced in the Emx1-expressing lineage. J Neurosci *22*, 6309-6314. 20026564.
3. Luo, L., Ambrozkiewicz, M.C., Benseler, F., Chen, C., Dumontier, E., Falkner, S., Furlanis, E., Gomez, A.M., Hoshina, N., Huang, W.H., et al. (2020). Optimizing Nervous System-Specific Gene Targeting with Cre Driver Lines: Prevalence of Germline Recombination and Influencing Factors. Neuron *106*, 37-65 e35. 10.1016/j.neuron.2020.01.008.
4. Drapeau, E., Riad, M., Kajiwara, Y., and Buxbaum, J.D. (2018). Behavioral Phenotyping of an Improved Mouse Model of Phelan-McDermid Syndrome with a Complete Deletion of the Shank3 Gene. eNeuro *5*. 10.1523/ENEURO.0046-18.2018.
5. Karczewski, K.J., Francioli, L.C., Tiao, G., Cummings, B.B., Alfoldi, J., Wang, Q., Collins, R.L., Laricchia, K.M., Ganna, A., Birnbaum, D.P., et al. (2020). The mutational constraint spectrum quantified from variation in 141,456 humans. Nature *581*, 434-443. 10.1038/s41586-020-2308-7.
6. Deciphering Developmental Disorders Study (2017). Prevalence and architecture of de novo mutations in developmental disorders. Nature *542*, 433-438. 10.1038/nature21062.
7. Fu, J.M., Satterstrom, F.K., Peng, M., Brand, H., Collins, R.L., Dong, S., Klei, L., Stevens, C.R., Cusick, C., Babadi, M., et al. (2021). Rare coding variation illuminates the allelic architecture, risk genes, cellular expression patterns, and phenotypic context of autism. medRxiv, 2021.2012.2020.21267194. 10.1101/2021.12.20.21267194.
8. Epi, K.c., and Epilepsy Phenome/Genome, P. (2017). Ultra-rare genetic variation in common epilepsies: a case-control sequencing study. Lancet Neurol *16*, 135-143. 10.1016/S1474-4422(16)30359-3.

9. Heyne, H.O., Singh, T., Stamberger, H., Abou Jamra, R., Caglayan, H., Craiu, D., De Jonghe, P., Guerrini, R., Helbig, K.L., Koeleman, B.P.C., et al. (2018). De novo variants in neurodevelopmental disorders with epilepsy. Nat Genet *50*, 1048-1053. 10.1038/s41588-018-0143-7.

10. Epi25 Collaborative. Electronic address, s.b.u.e.a., and Epi, C. (2019). Ultra-Rare Genetic Variation in the Epilepsies: A Whole-Exome Sequencing Study of 17,606 Individuals. American journal of human genetics *105*, 267-282. 10.1016/j.ajhg.2019.05.020.

11. Darnell, J.C., Van Driesche, S.J., Zhang, C., Hung, K.Y., Mele, A., Fraser, C.E., Stone, E.F., Chen, C., Fak, J.J., Chi, S.W., et al. (2011). FMRP stalls ribosomal translocation on mRNAs linked to synaptic function and autism. Cell *146*, 247-261. 10.1016/j.cell.2011.06.013.

12. Weyn-Vanhentenryck, S.M., Mele, A., Yan, Q., Sun, S., Farny, N., Zhang, Z., Xue, C., Herre, M., Silver, P.A., Zhang, M.Q., et al. (2014). HITS-CLIP and integrative modeling define the Rbfox splicing-regulatory network linked to brain development and autism. Cell Rep *6*, 1139-1152. 10.1016/j.celrep.2014.02.005.

13. Wagnon, J.L., Briese, M., Sun, W., Mahaffey, C.L., Curk, T., Rot, G., Ule, J., and Frankel, W.N. (2012). CELF4 regulates translation and local abundance of a vast set of mRNAs, including genes associated with regulation of synaptic function. PLoS Genet *8*, e1003067. 10.1371/journal.pgen.1003067.

14. De Rubeis, S., He, X., Goldberg, A.P., Poultney, C.S., Samocha, K., Cicek, A.E., Kou, Y., Liu, L., Fromer, M., Walker, S., et al. (2014). Synaptic, transcriptional and chromatin genes disrupted in autism. Nature *515*, 209-215. 10.1038/nature13772.

15. Tukiainen, T., Villani, A.C., Yen, A., Rivas, M.A., Marshall, J.L., Satija, R., Aguirre, M., Gauthier, L., Fleharty, M., Kirby, A., et al. (2017). Landscape of X chromosome inactivation across human tissues. Nature *550*, 244-248. 10.1038/nature24265.

16. Oliva, M., Munoz-Aguirre, M., Kim-Hellmuth, S., Wucher, V., Gewirtz, A.D.H., Cotter, D.J., Parsana, P., Kasela, S., Balliu, B., Vinuela, A., et al. (2020). The impact of sex on gene expression across human tissues. Science *369*. 10.1126/science.aba3066.

Supplementary Figure 1

A

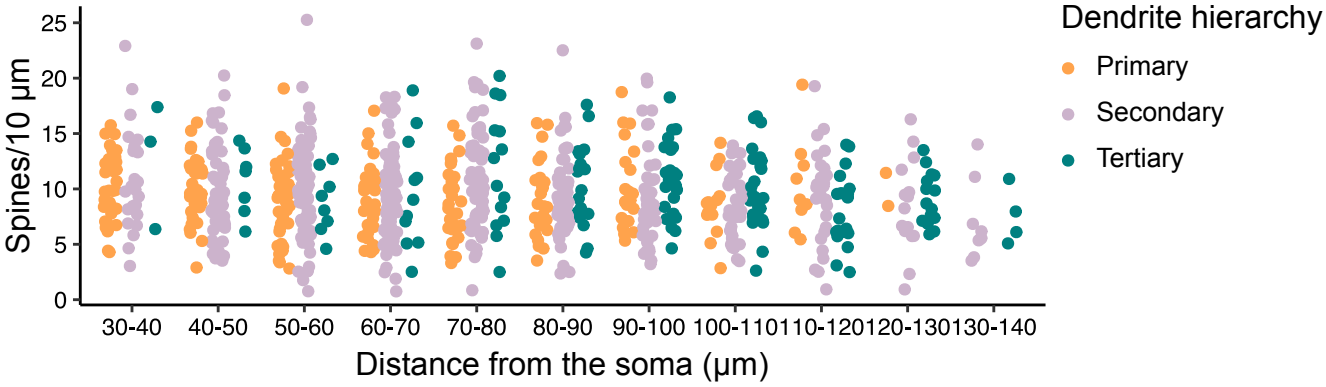

B

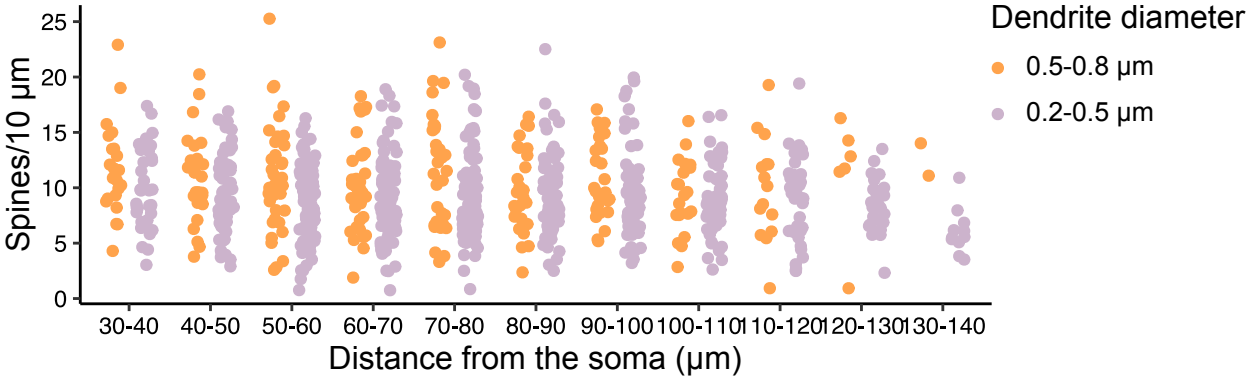

C

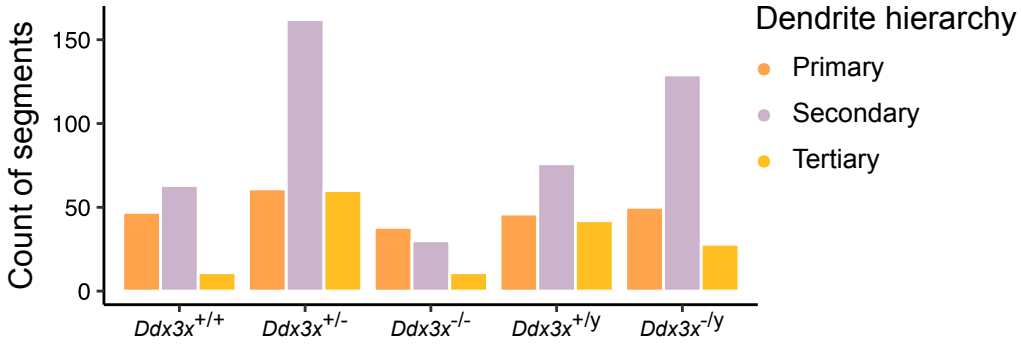

D

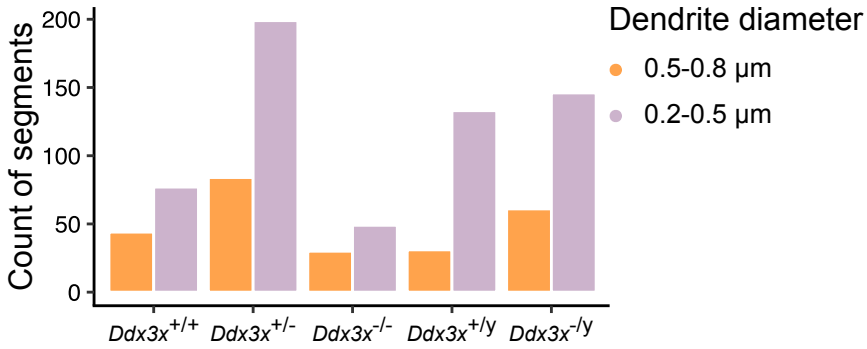

Supplementary Figure 2

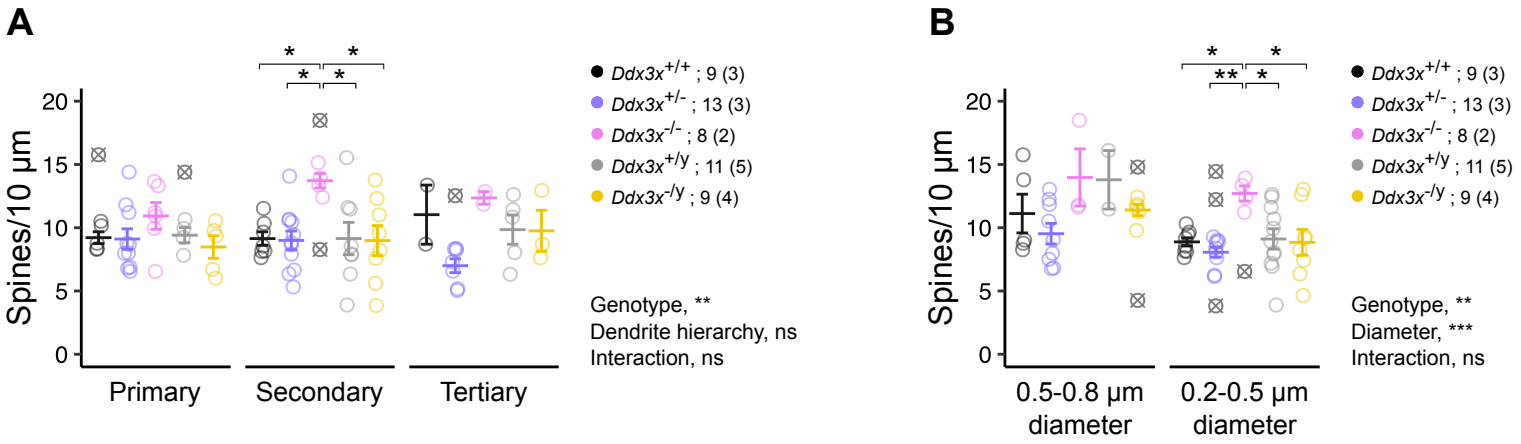

Supplementary Figure 3

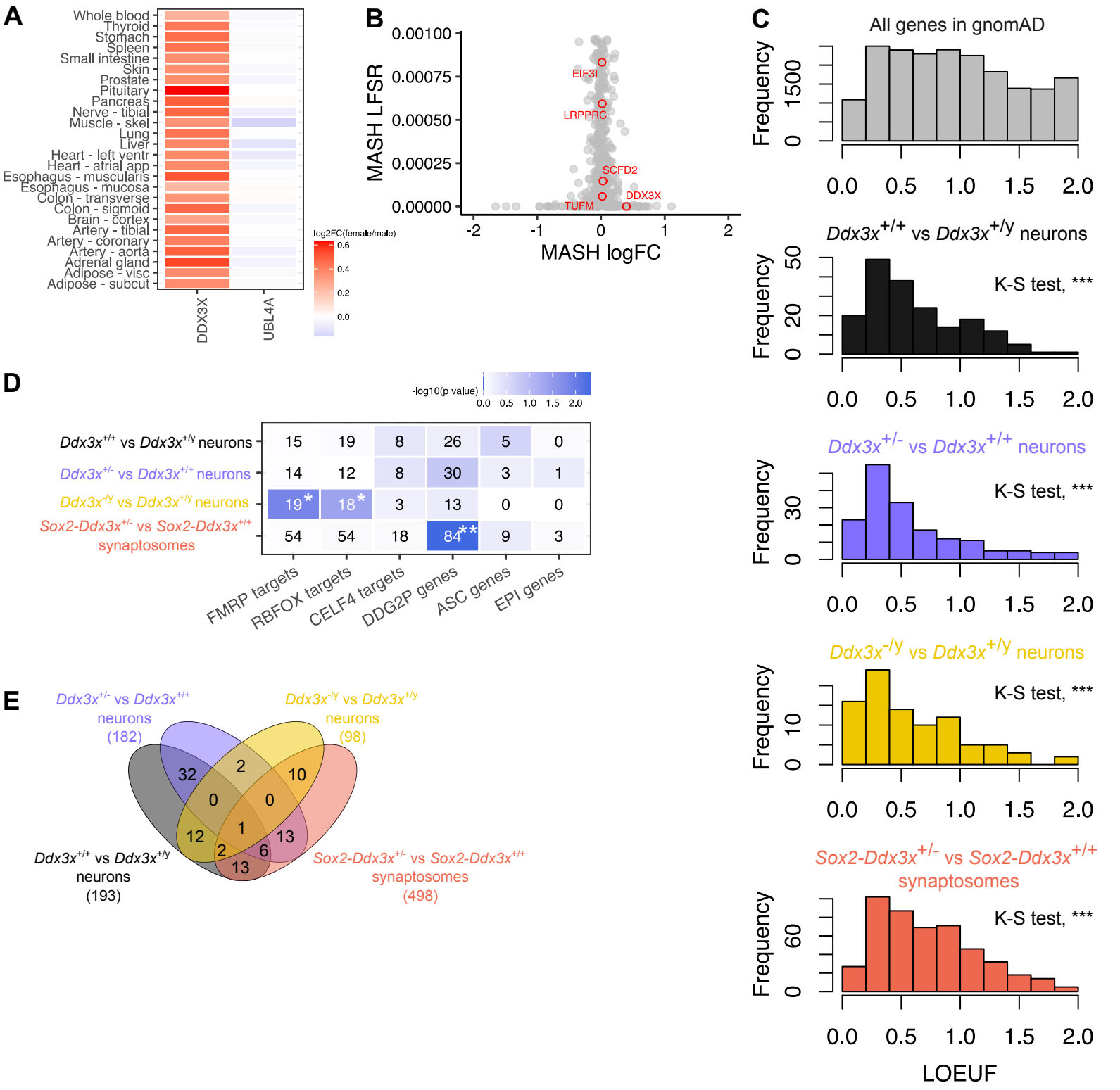

Supplementary Figure 4

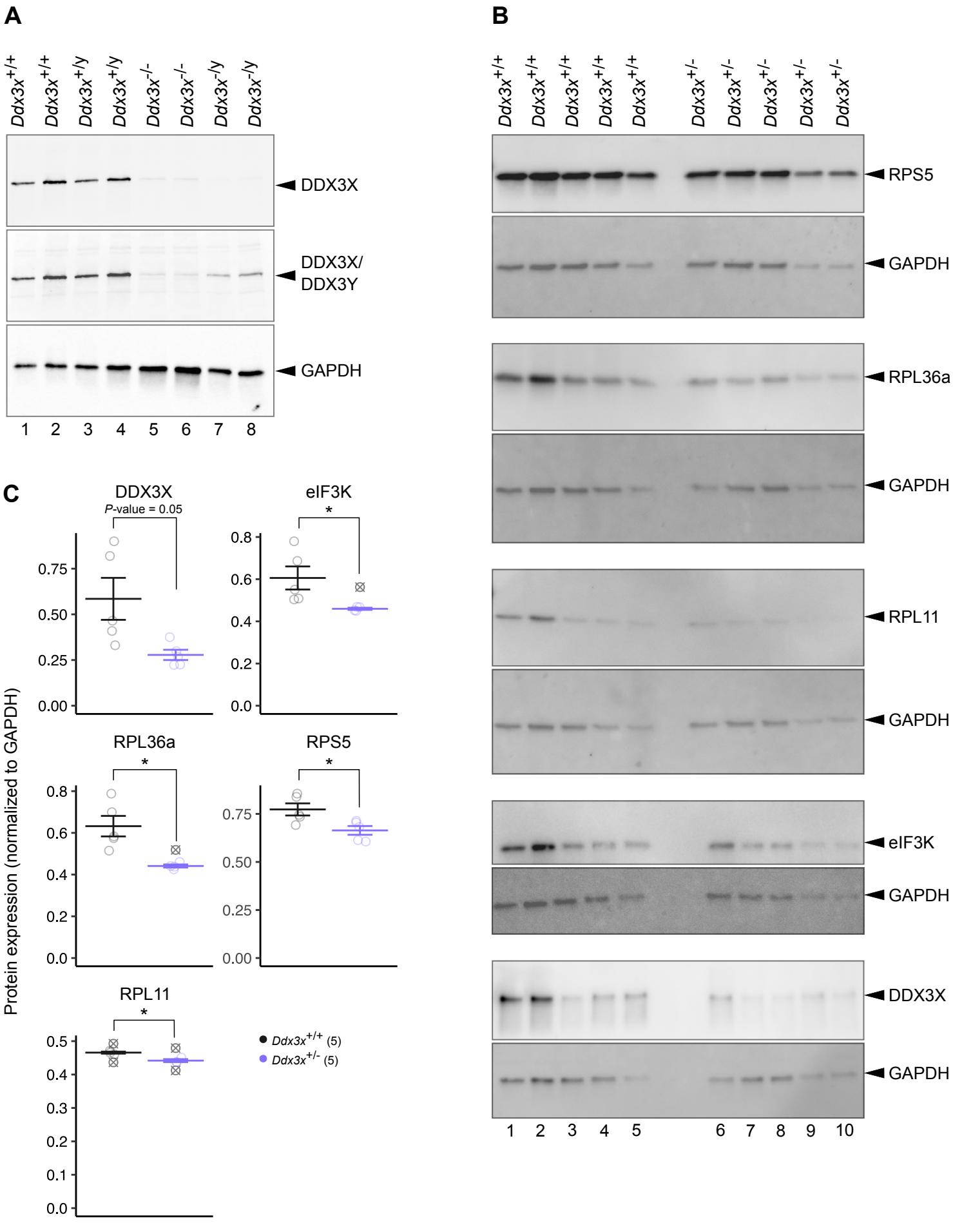

Supplementary Figure 5

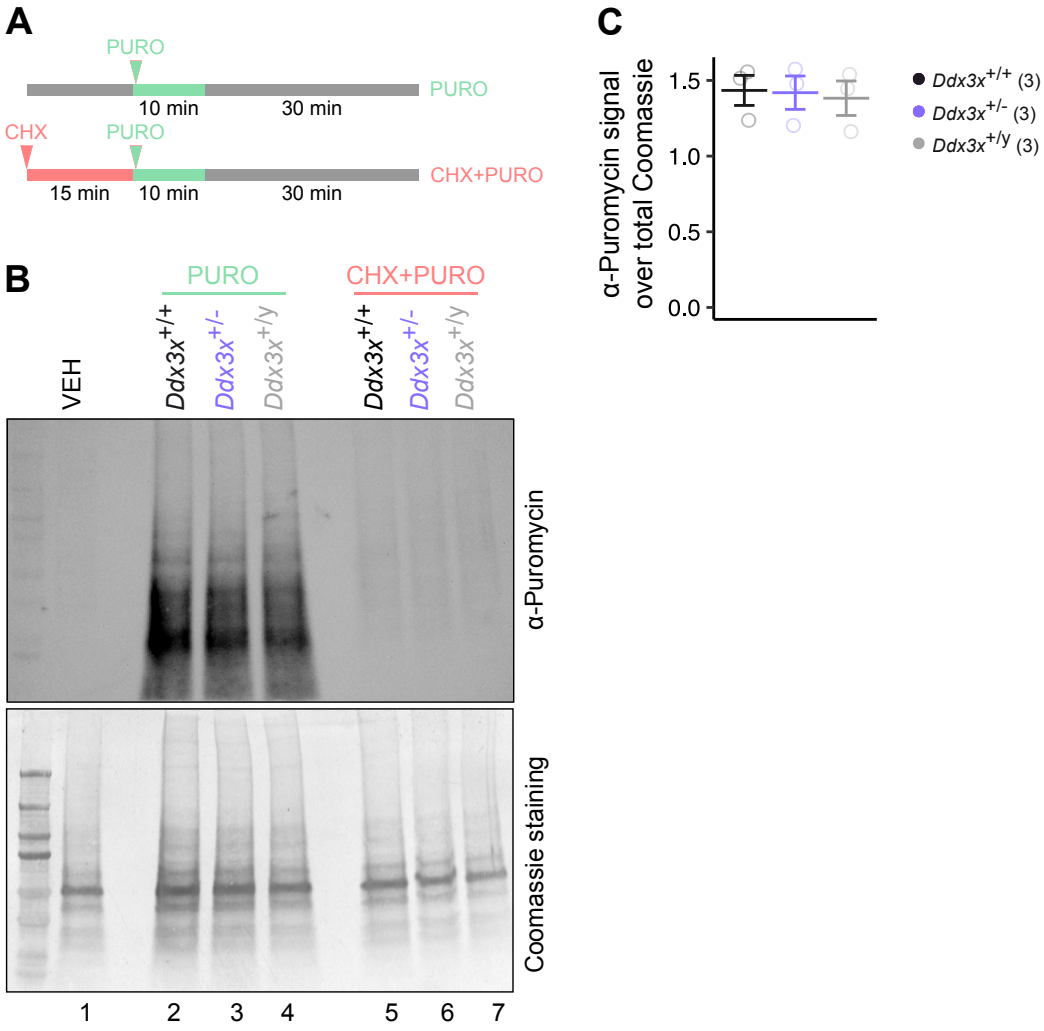

Supplementary Figure 6

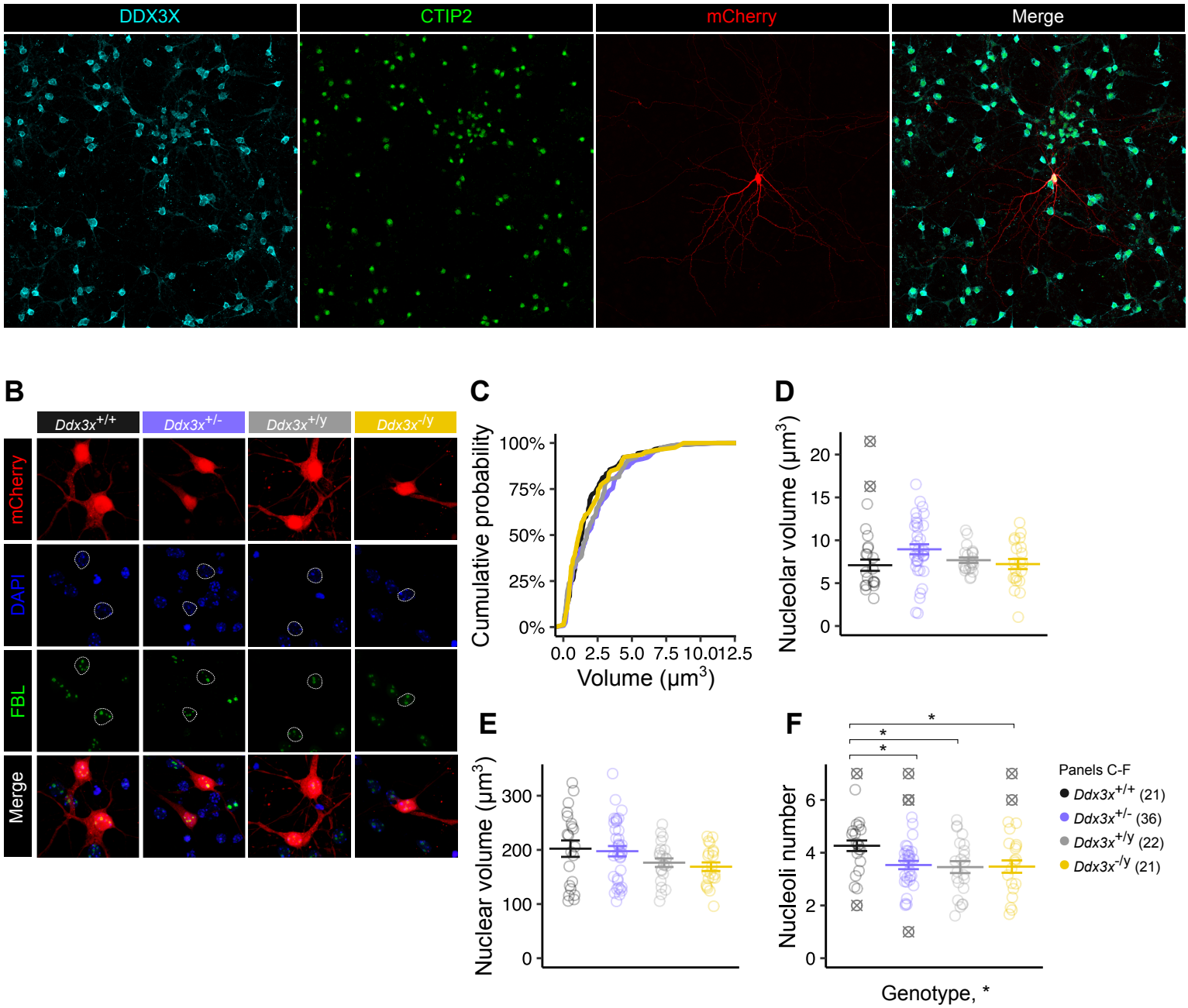

Supplementary Figure 7

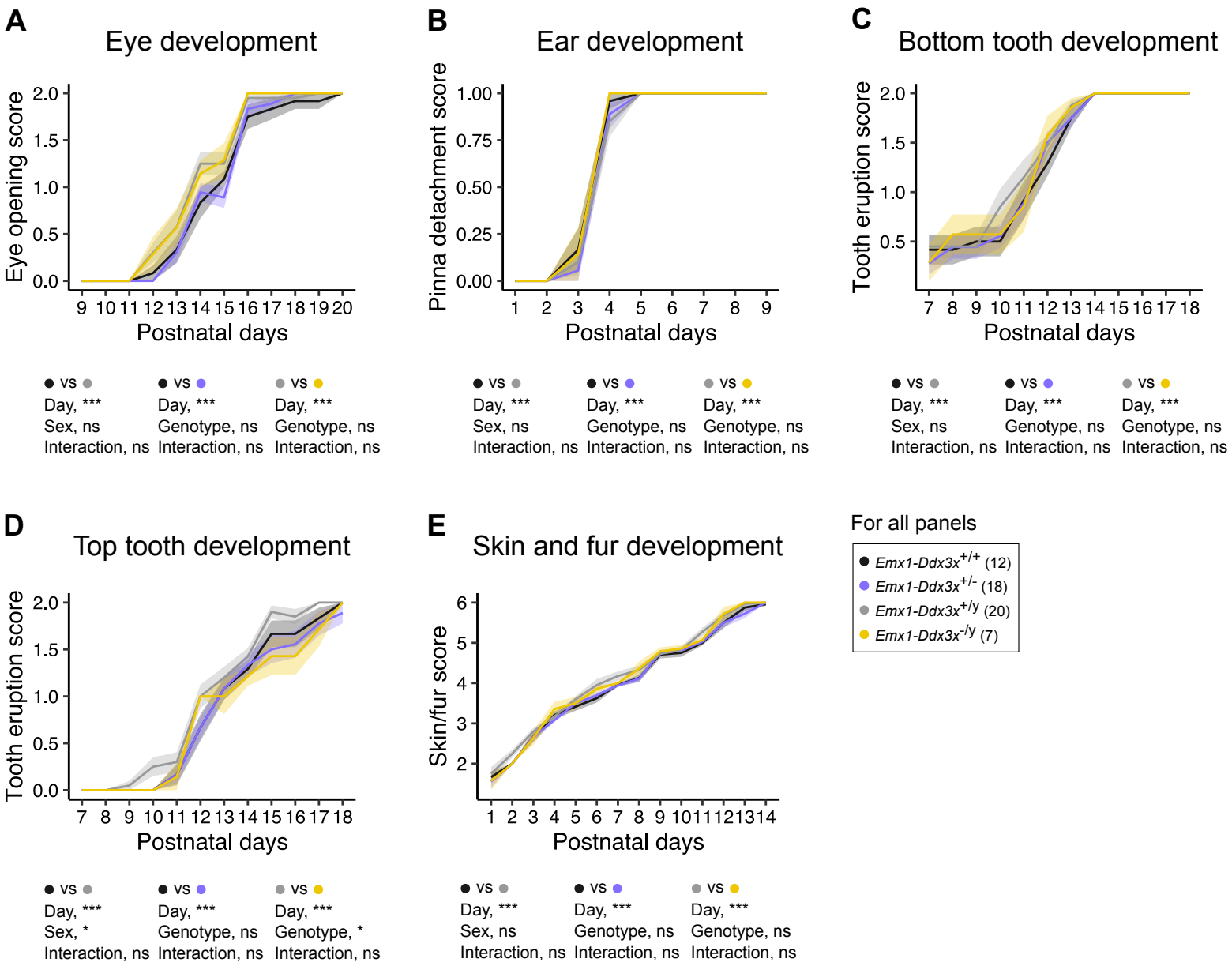

Supplementary Figure 8

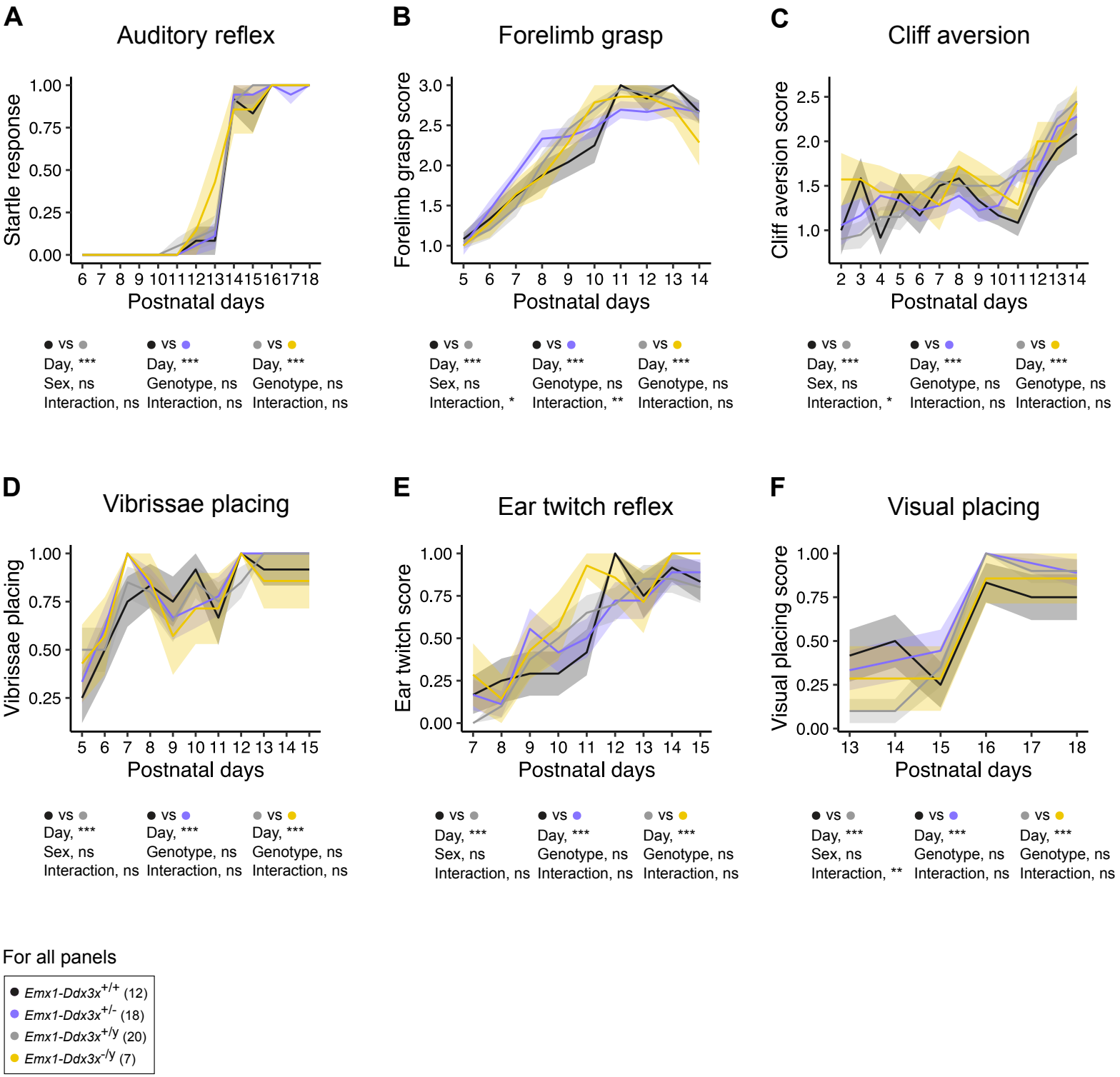

Supplementary Figure 9

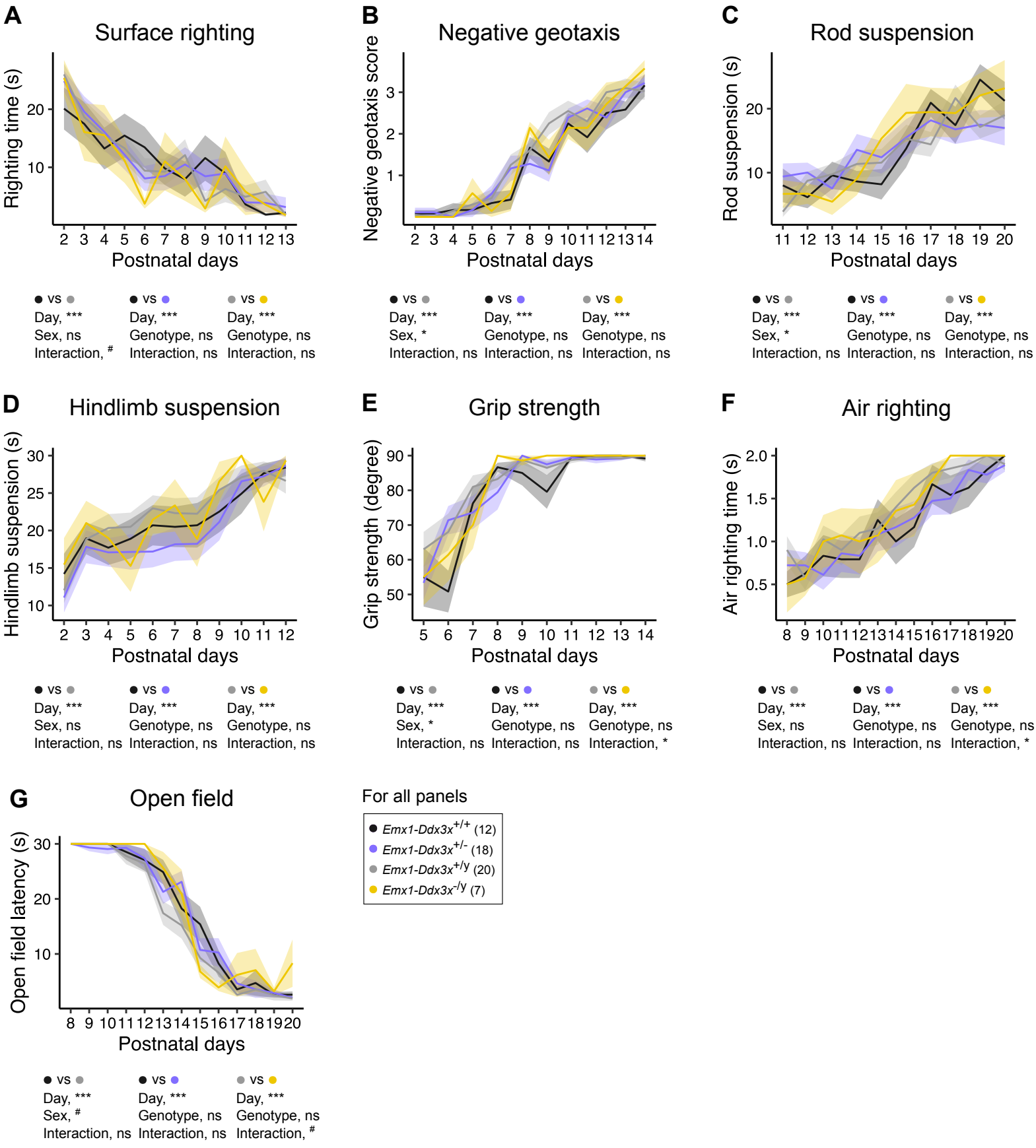

Supplementary Figure 10

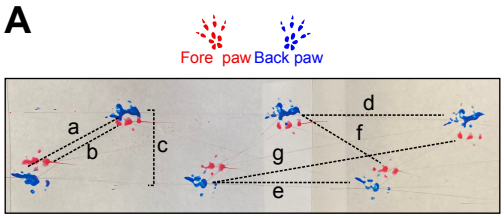

B, Distance between back paws
C, Distance between fore paws
D, Sway distance
E, Left stride
F, Right stride
G, Left fore paw to right back paw diagonal
H, Right fore paw to left back paw diagonal

For all panels

P19, P22	P30
Emx1-Ddx3x$^{+/+}$ (19)	*Emx1-Ddx3x*$^{+/+}$ (16)
Emx1-Ddx3x$^{+/-}$ (10)	*Emx1-Ddx3x*$^{+/-}$ (8)
Emx1-Ddx3x$^{+/y}$ (14)	*Emx1-Ddx3x*$^{+/y}$ (9)
Emx1-Ddx3x$^{-/y}$ (15)	*Emx1-Ddx3x*$^{-/y}$ (12)

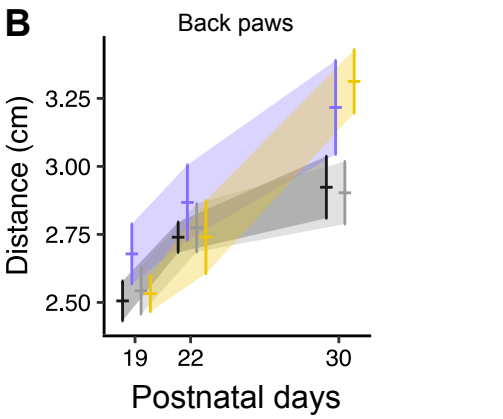

● vs ● Day, *** Sex, ns Interaction, ns
● vs ● Day, *** Genotype, * Interaction, ns
● vs ● Day, *** Genotype, ns Interaction, #

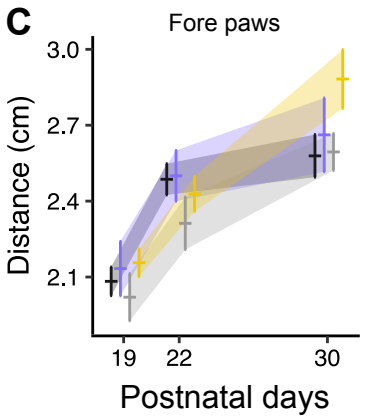

● vs ● Day, *** Sex, ns Interaction, ns
● vs ● Day, *** Genotype, ns Interaction, ns
● vs ● Day, *** Genotype, ** Interaction, ns

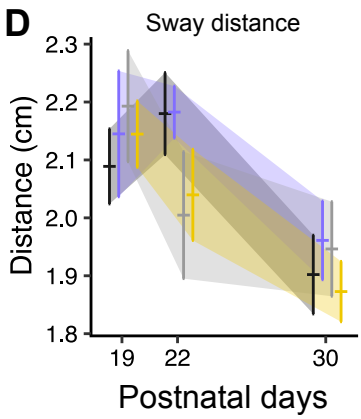

● vs ● Day, * Sex, ns Interaction, ns
● vs ● Day, ** Genotype, ns Interaction, ns
● vs ● Day, ** Genotype, ns Interaction, ns

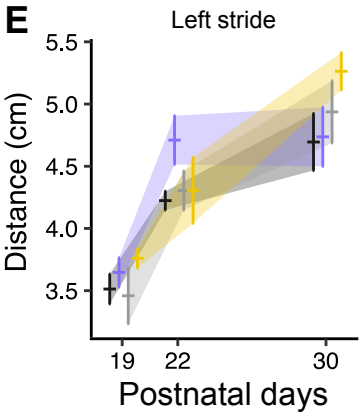

● vs ● Day, *** Sex, ns Interaction, ns
● vs ● Day, *** Genotype, # Interaction, ns
● vs ● Day, *** Genotype, ns Interaction, ns

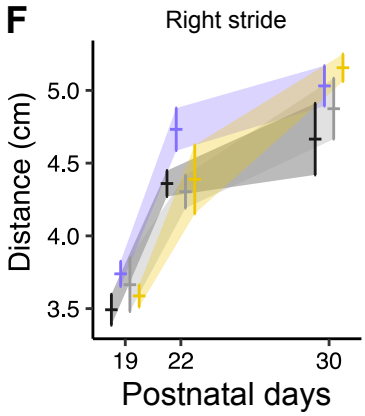

● vs ● Day, *** Sex, ns Interaction, ns
● vs ● Day, *** Genotype, * Interaction, ns
● vs ● Day, *** Genotype, ns Interaction, ns

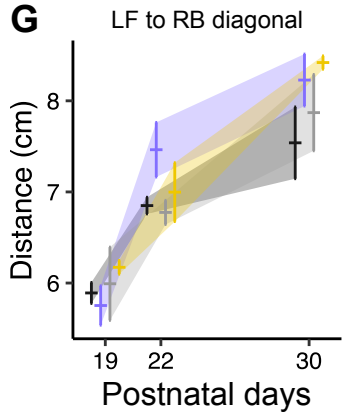

● vs ● Day, *** Sex, ns Interaction, ns
● vs ● Day, *** Genotype, ns Interaction, ns
● vs ● Day, *** Genotype, ns Interaction, ns

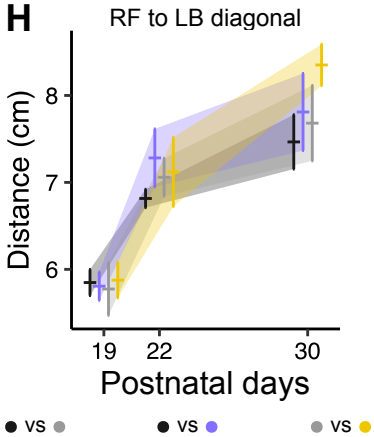

● vs ● Day, *** Sex, ns Interaction, ns
● vs ● Day, *** Genotype, ns Interaction, ns
● vs ● Day, *** Genotype, ns Interaction, ns

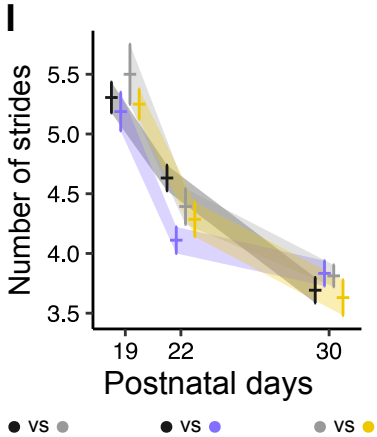

● vs ● Day, *** Sex, ns Interaction, ns
● vs ● Day, *** Genotype, * Interaction, ns
● vs ● Day, *** Genotype, # Interaction, ns

Supplementary Figure 11

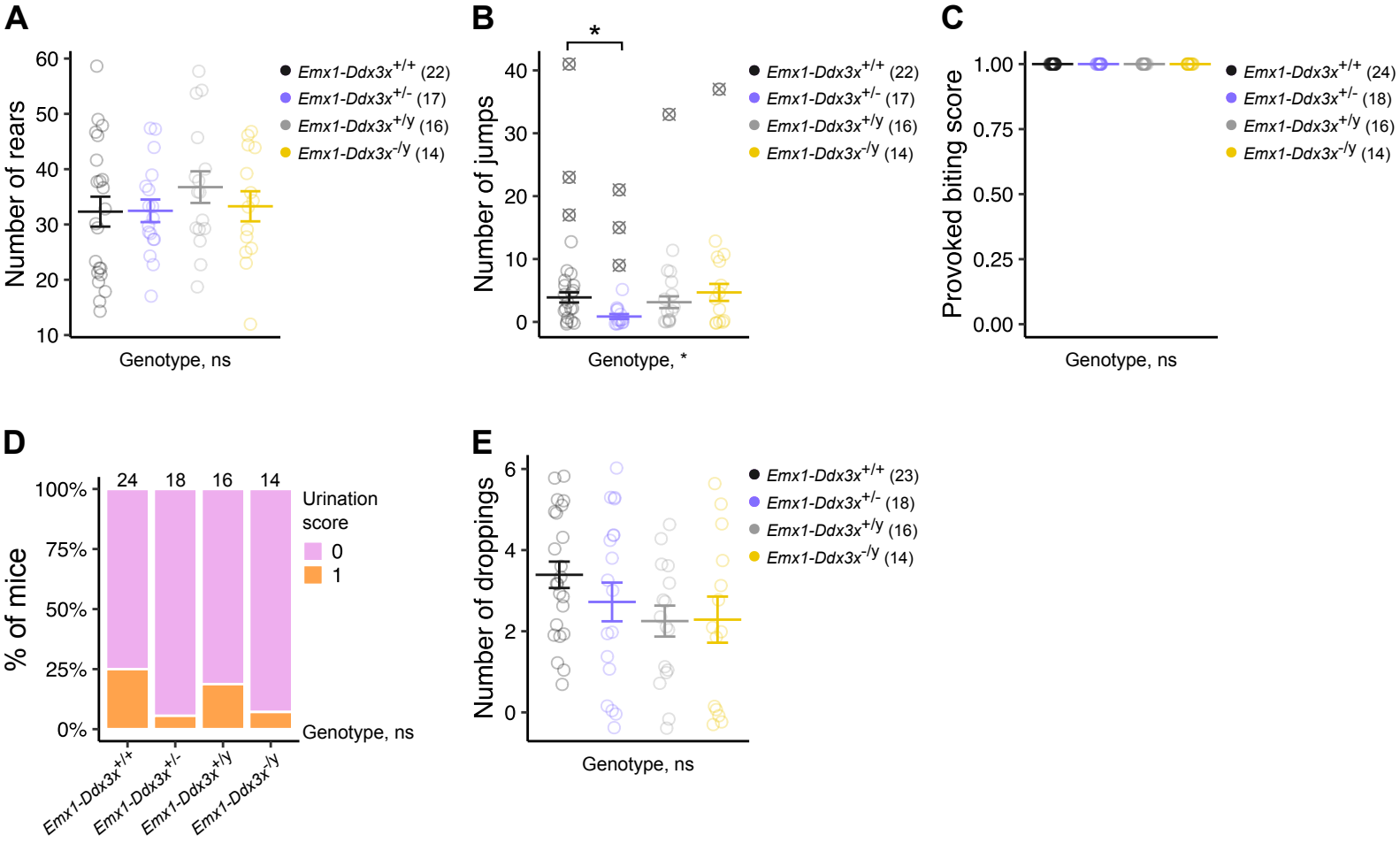

Supplementary Figure 12

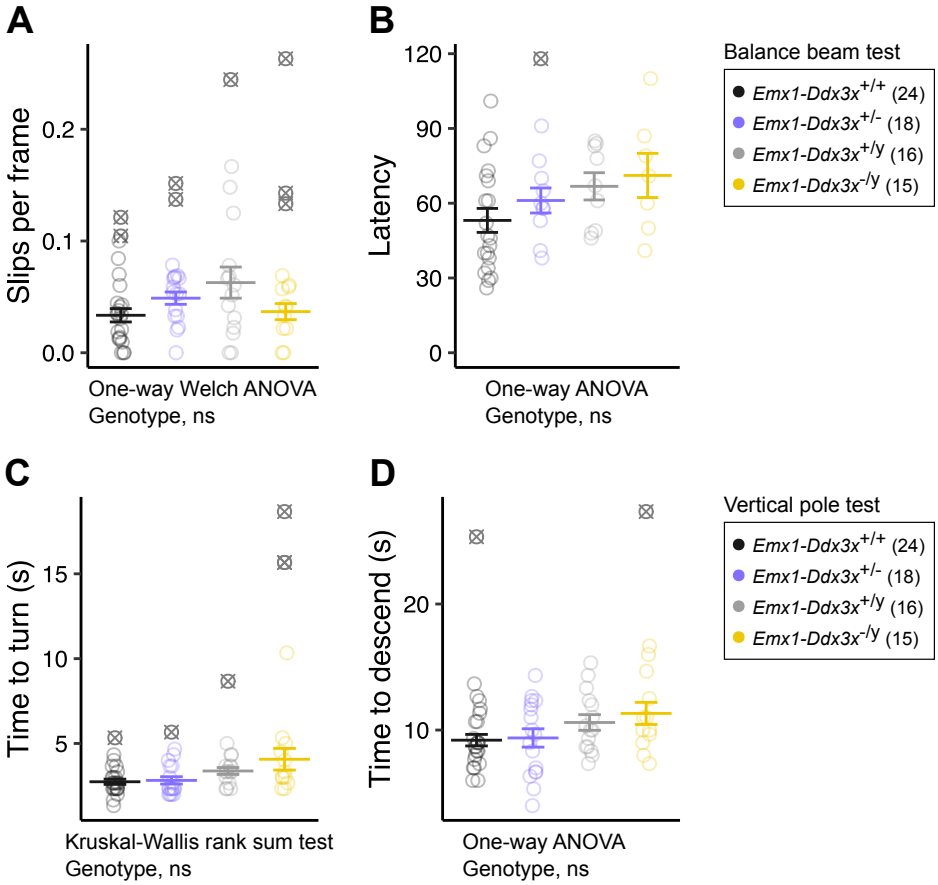

Source data for Supplementary Figure 4A

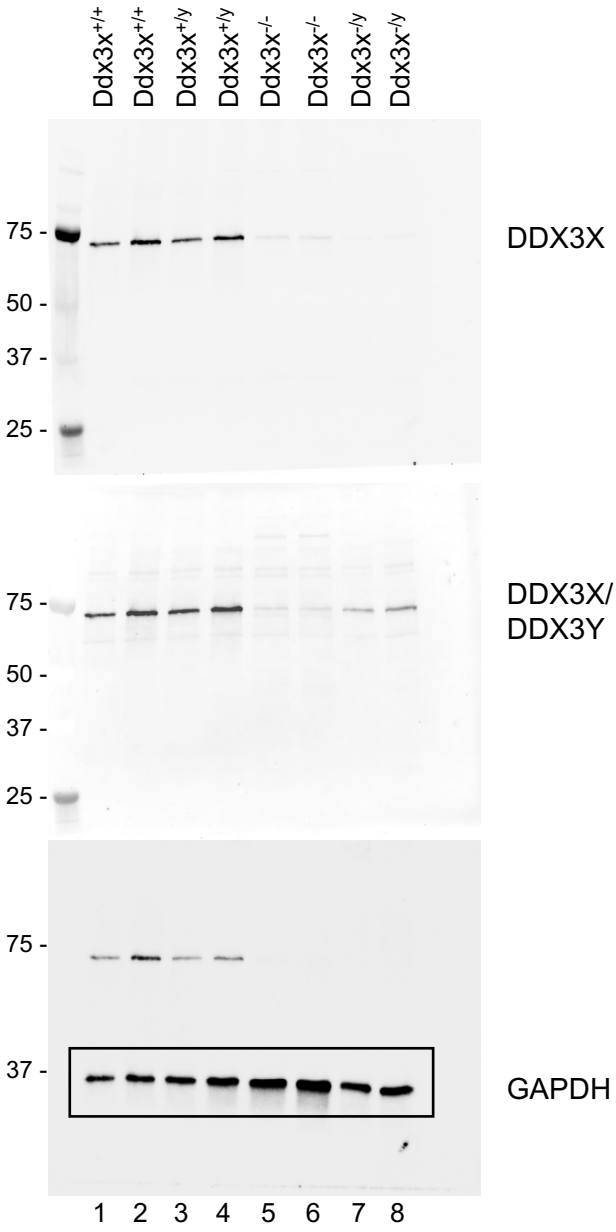

Source data for Supplementary Figure 4B